Direct Observation of Systematic Deviations from the Bethe Stopping Theory for Relativistic Heavy Ions

C. Scheidenberger,[1] H. Geissel,[1] H. H. Mikkelsen,[2] F. Nickel,[1] T. Brohm,[3] H. Folger,[1] H. Irnich,[1] A. Magel,[4] M. F. Mohar,[1] G. Münzenberg,[1] M. Pfützner,[1] E. Roeckl,[1] I. Schall,[1] D. Schardt,[1] K.-H. Schmidt,[1] W. Schwab,[1] M. Steiner,[3] Th. Stöhlker,[1] K. Sümmerer,[1] D. J. Vieira,[1] B. Voss,[3] and M. Weber[1]

[1]*Gesellschaft für Schwerionenforschung Darmstadt, Planckstrasse 1, D-64291 Darmstadt, Germany*
[2]*Odense Universitet, DK-5230 Odense, Germany*
[3]*Technische Hochschule Darmstadt, Schlossgartenstrasse 9, D-64289 Darmstadt, Germany*
[4]*Universitat Giessen, Heinrich-Buff-Ring 16, D-35392 Giessen, Germany*

(Received 15 February 1994)

The SIS accelerator facilities at GSI in combination with a magnetic spectrometer allow the direct measurement of stopping powers for relativistic heavy ions up to uranium with high precision for the first time. Here, we report on representative results obtained for projectiles up to xenon in the energy range from 700 to 1000 MeV/u. Systematic deviations from the Bethe stopping-power theory are observed, whereas the data are in good agreement with theory once Mott and Bloch corrections and the Fermi density effect are included.

PACS numbers: 34.50.Bw

The first experimental results on the penetration of swift heavy ions through matter were obtained with fission fragments [1]. New accelerators have extended the energy range up to the GeV/u region and provide highly stripped ions of all elements. It is obvious that under these conditions the complexity due to unknown charge-state evolutions is strongly reduced.

At the BEVALAC accelerator in Berkeley, pioneering experiments on the stopping of relativistic heavy ions in matter were carried out [2–5]. The experimental and theoretical results are summaried in Ref. [6]. In these experiments ranges in solids were measured for several projectiles, e.g., ^{56}Fe and ^{238}U with 600 and 955 MeV/u incident energies, respectively, using an emulsion tracking method. Because only one fixed energy was used in each measurement, these range results were interpreted in terms of integrated stopping powers as provided by the Bethe formula with higher-order corrections. This procedure is affected by several ambiguities: The charge-state evolution of the projectiles during the complete slowing down was approximated by an effective charge state using a simple expression [7]. However, the important dependence on the target material was neglected. This analysis would require the knowledge of the velocity dependence of all higher-order terms and the limits of their validity. Nuclear reactions have to be considered for relativistic heavy ions particularly if they are stopped in light target material. For example, for 600 MeV/u ^{56}Fe ions stopped in carbon more than 70% of the projectiles experience nuclear reactions [8]. These reactions are dominated by peripheral collisions where only few nucleons are removed from the projectile. However, those reaction products cannot be resolved by the track method. Because of these experimental limitations and the high level of accuracy required to verify the theoretical higher-order terms in stopping, it is understandable that these early measurements led to controversial conclusions [4,9].

We measured stopping powers of relativistic heavy ions in transmission geometry using thin targets, where the relative energy loss is small, the ionic charge state is well known, and an unambiguous particle identification is applied. Our results are compared with theoretical predictions.

The heavy-ion synchrotron SIS [10] at GSI can accelerate ions of all elements up to a maximum magnetic rigidity of 18 Tm. Here we present experimental stopping-power data for 702 MeV/u ^{18}O, 1000 MeV/u ^{40}Ar, 1000 MeV/u ^{86}Kr, and 800 MeV/u ^{136}Xe ions impinging on various solids. The absolute energy of the incident ions was determined by the measurement of the revolution frequency in the synchrotron with an accuracy of better than 4×10^{-4}. The beams were injected into the FRS [11], a magnetic forward spectrometer with high resolution. They passed a 4.5 mg/cm^2 Ti foil and in the case of O, Ar, and Kr an additional 8.9 mg/cm^2 Al foil before penetrating through the target. The targets were made of Be, C, Al, Cu, and Pb in the thickness range of 200 to 8000 mg/cm^2. The thicknesses and nonuniformities were determined by means of an optomechanical method [12]. The target-thickness fluctuations were only a few microns, which is an essential prerequisite for precise stopping-power measurements in this energy range. The targets were placed at the entrance of the FRS which consists of four independent ion-optical stages. At each focal plane, remotely movable multiwire proportional chambers with a position resolution of about 0.5 mm are mounted. The measured position spectra were transformed into energy spectra using the dispersion and the measured magnetic field strengths. In the range of target thicknesses used in this experiment, the shape of these spectra is Gaussian and we obtained the most probable energy loss from fitting the distributions. The energy

0031-9007/94/73(1)/50(4)$06.00

measurement was performed with a resolution of 10^{-4} at the midfocal plane characterized by a dispersion of 6.8 cm/%. An unambiguous particle identification with respect to the ion's atomic number Z_1 and mass A_1 after the penetration through the target can be performed at the final focal plane with our standard detectors to discriminate nuclear reaction products [13].

The stopping power was extracted from the measured energy losses applying numerical differentiation of the fitted energy-loss–thickness relations. The experimental errors of about 2% result from the uncertainty of the incident beam energy, the measured magnetic rigidity, and thickness uncertainties of the target. For the heavier ions like Kr and Xe the errors are about 1% in the same targets since the contribution of the energy-loss uncertainty decreases.

In addition to the stopping power, the charge-state distributions have been measured simultaneously [14,15] to determine the contribution of the charge-state evolution inside the targets to the stopping-power results. In the worst case for Xe ions in the thinnest targets this contribution is less than 1%, for the thicker targets it decreases to 2×10^{-3}, and for the lighter projectiles it is completely negligible.

The slowing down of swift heavy ions is dominated by the energy transfer to the atomic electrons. Under the assumption of a fully stripped ion the stopping power of the medium is given by

$$\frac{dE}{dx}=\frac{4\pi(Z_1e^2)^2}{mc^2\beta^2}NL\,, \tag{1}$$

where N is the number of electrons per unit volume in the target, m and e are the electron rest mass and unit charge, respectively, β is the velocity of the particle relative to the speed of light c, and L is the dimensionless stopping number to be specified.

At relativistic velocities L can be expanded according to

$$L=L_0+\Delta L\,, \tag{2}$$

where L_0 is based on the first Born approximation, i.e., quantal perturbation theory to first order, and ΔL accounts for various higher-order terms. The relative importance of the two terms in (2) is determined by the magnitude of $Z_1\alpha/\beta$, where α is the fine structure constant. Only in the limit of $Z_1\alpha/\beta \ll 1$ is the stopping well described by L_0 alone.

Within the first Born approximation the relativistic stopping number is given by [16]

$$L_0=\ln\left(\frac{2mc^2\beta^2}{I}\right)-\ln(1-\beta^2)-\beta^2-\delta/2\,. \tag{3}$$

The first term in Eq. (3) is the nonrelativistic Bethe logarithm defined in terms of the mean excitation energy I [17], and the following two terms are relativistic corrections that mainly arise from kinematic changes in the scattering process [18]. The Fermi density effect, $-\delta/2$, accounts for the dielectric polarization of the stopping medium at relativistic velocities [19]. Shell corrections accounting for the binding of the target electrons and the Barkas term caused by the displacement of the electrons during the collision are both negligible in the considered velocity range [16,20].

For relativistic heavy ions ΔL must be considered. As shown by Bloch [21], the correction

$$\Delta L_{\text{Bloch}}=\psi(1)-\mathrm{Re}\,\psi(1+iZ_1\alpha/\beta) \tag{4}$$

has to be added to the first Born approximation for all velocities, where ψ is the logarithmic derivative of the gamma function in the complex plane. This term takes into account the saturation of energy transfer in small-impact-parameter collisions and thus reduces the Bethe prediction.

Second, the relativistic Mott scattering must be considered [22]. We included ΔL_{Mott} by integrating the exact Mott cross sections over all scattering angles, whereas approximate expressions have been given by Ahlen [7]. Since we used the exact Mott cross sections, the relativistic Bloch correction proposed by Ahlen [23] is not included in our model.

For the stopping of relativistic heavy ions we thus arrive at the rather simple expression

$$L=L_0+\Delta L_{\text{Bloch}}+\Delta L_{\text{Mott}}\,, \tag{5}$$

which is the Bethe-Bloch formula corrected for Mott scattering and the density effect.

In Fig. 1 the velocity dependence of the terms in (5) is shown for the case of fully stripped Xe ions in an aluminum target. The I values and Fermi density corrections are taken from Refs. [24,25]. Note that the Mott correction is the dominating correction increasing with projectile velocity, whereas the relevance of the Bloch term decreases.

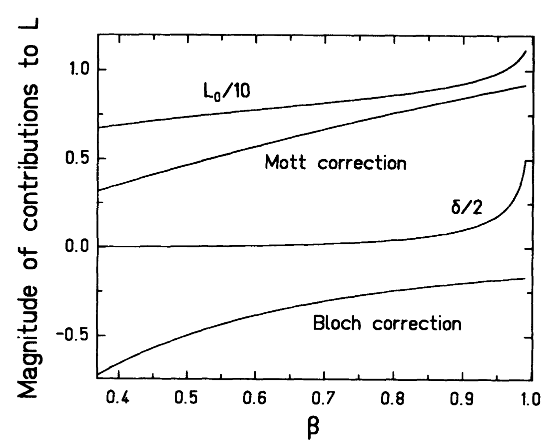

FIG. 1. Magnitude of the contributions to the stopping number for xenon ions in aluminum as a function of the projectile velocity.

TABLE I. Experimental stopping-power values for different projectile-target combinations in MeV/(mg/cm^2) compared with the theoretical predictions from Eqs. (3) and (5).

Projectile	Target	Eq. (3)	Eq. (5)	Experiment
$^{18}_{8}$O	Be	0.125	0.126	0.125 ± 0.002
690 MeV/u	C	0.137	0.138	0.138 ± 0.004
(β=0.819)	Al	0.123	0.124	0.123 ± 0.004
	Pb	0.083	0.084	0.084 ± 0.002
$^{40}_{18}$Ar	Be	0.574	0.585	0.578 ± 0.016
985 MeV/u	C	0.629	0.641	0.640 ± 0.019
(β=0.874)	Al	0.569	0.581	0.584 ± 0.019
	Cu	0.494	0.505	0.494 ± 0.016
	Pb	0.386	0.396	0.389 ± 0.012
$^{86}_{36}$Kr				
900 MeV/u	Be	2.346	2.438	2.432 ± 0.037
(β=0.861)				
$^{136}_{54}$Xe	Be	5.488	5.812	5.861 ± 0.076
780 MeV/u	C	6.014	6.378	6.524 ± 0.084
(β=0.839)	Al	5.404	5.755	5.806 ± 0.121
	Cu	4.703	5.036	5.077 ± 0.066
	Pb	3.654	3.942	3.959 ± 0.063

Below the predictions of our model, Eq. (5), will be compared with the experimental results.

A unique feature of the present measurements is the fact that the ions up to Xe are fully ionized during their penetration through the targets. Therefore the comparison of experimental stopping powers with theoretical predictions is not complicated by considerations of charge-changing processes. Table I shows the investigated projectile-target combinations and the measured stopping powers in comparison with theoretical predictions in units of MeV/(mg/cm^2).

In Fig. 2 the comparison of theory with experiment is shown for the different projectiles in various target materials with atomic number Z_2. The predictions of Eqs. (3) (open squares) and (5) (full circles) are divided by the experimental values. Since the velocity varies only slightly for the different projectiles, the observed deviation from Bethe theory is due to the increasing projectile atomic number.

For the light projectiles, e.g., O and Ar, the measured stopping powers agree well with both the Bethe formula and the extended theory. Similar results were observed at lower energies [26–28]. For high-Z ions the first Born approximation is no longer applicable, which explains the failure of the Bethe theory. This is clearly demonstrated by systematic deviations of about 3% and 7% for the Kr and Xe data, respectively. However, the comparison between the experimental and calculated data confirms the importance of the Mott and Bloch corrections in the considered velocity range.

Our investigations will be extended up to the heaviest ions in forthcoming experiments.

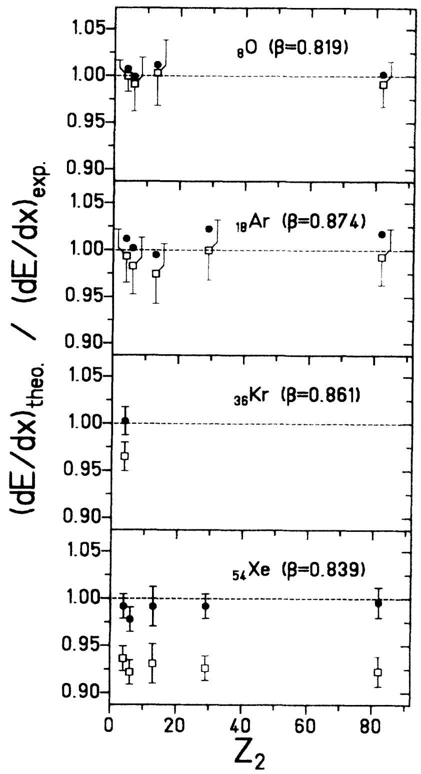

FIG. 2. Ratio of calculated and measured stopping powers for different projectile-target combinations. The theoretical predictions of Eqs. (3) (open squares) and (5) (full circles) are divided by the experimental values. Not all error bars are shown for the sake of clarity. For the heavier projectiles systematic deviations from the Bethe theory are observed, but for all data points good agreement with our theoretical description is found. The dashed lines are to guide the eye.

In summary, for the first time direct stopping-power measurements have been performed to high precision with bare relativistic heavy ions up to Xe. Since the projectiles are fully ionized, no complications due to charge-exchange processes obscure the direct comparison with theory. The importance of the Bloch and Mott higher-order-correction terms to the relativistic Bethe formula is demonstrated. Our calculations [Eq. (5)] predict the stopping power of fully ionized relativistic heavy ions up to Xe correctly within the experimental errors.

We would like to thank the FRS technicians, the GSI accelerator staff, and the members of the target laboratory for their excellent support. Fruitful discussions with P. Sigmund are gratefully acknowledged. The work of H.H.M. was supported by the Danish Natural Science Research Council. Another of us, D.J.V., wishes to acknowledge support from the Alexander von Humboldt Foundation.

[1] N. O. Lassen, Mat. Fys. Medd. Dan. Vidensk. Selsk. **26**,

5 (1951); **26**, 12 (1951).
[2] G. Tarlé and M. Solarz, Phys. Rev. Lett. **41**, 483 (1978).
[3] M. H. Salamon, S. P. Ahlen, G. Tarlé, and K. C. Crebbin, Phys. Rev. A **23**, 73 (1981).
[4] S. P. Ahlen and G. Tarle, Phys. Rev. Lett. **50**, 1110 (1983).
[5] C. J. Waddington, D. J. Fixsen, and P. S. Freier, Phys. Rev. A **32**, 3102 (1985).
[6] S. P. Ahlen, Rev. Mod. Phys. **52**, 121 (1980).
[7] S. P. Ahlen, Phys. Rev. A **17**, 1236 (1978).
[8] S. Kox *et al.*, Phys. Lett. B **159**, 15 (1985).
[9] C. J. Waddington *et al.*, Phys. Rev. A **34**, 3700 (1986).
[10] K. Blasche *et al.*, Part. Accel. **32**, 83 (1990).
[11] H. Geissel *et al.*, Nucl. Instrum. Methods Phys. Res., Sect. B **70**, 286 (1992).
[12] H. Folger *et al.*, Nucl. Instrum. Methods Phys. Res., Sect. A **303**, 24 (1991).
[13] B. Voss *et al.*, GSI Scientific Report No. 1991, GSI-92-1, 340, 1992 (unpublished).
[14] Th. Stöhlker *et al.*, Nucl. Instrum. Methods Phys. Res., Sect. B **61**, 408 (1991).
[15] C. Scheidenberger *et al.*, Nucl. Instrum. Methods Phys. Res., Sect. B (to be published).
[16] U. Fano, Annu. Rev. Nucl. Sci. **13**, 1 (1963).
[17] H. Bethe, Ann. Phys. (Leipzig) **5**, 325 (1930).
[18] C. Møller, Ann. Phys. (Leipzig) **14**, 531 (1932).
[19] E. Fermi, Phys. Rev. **57**, 485 (1940).
[20] J. D. Jackson and R. L. McCarthy, Phys. Rev. B **6**, 413 (1972).
[21] F. Bloch, Ann. Phys. (Leipzig) **16**, 285 (1933).
[22] N. F. Mott, Proc. R. Soc. (London) A **124**, 425 (1929).
[23] S. P. Ahlen, Phys. Rev. A **25**, 1856 (1982).
[24] R. M. Sternheimer, M. J. Berger, and S. M. Seltzer, At. Data Nucl. Data Tables **30**, 261 (1984).
[25] M. Inokuti and D. Y. Smith, Phys. Rev. B **25**, 61 (1982).
[26] B. Blank *et al.*, Nucl. Instrum. Methods Phys. Res., Sect. B **51**, 85 (1990).
[27] Th. Schwab *et al.*, Nucl. Instrum. Methods Phys. Res., Sect. B **48**, 69 (1990).
[28] R. Bimbot, Nucl. Instrum. Methods Phys. Res., Sect. B **69**, 1 (1992).